Available online at www.sciencedirect.com
SCIENCE DIRECT®
Energy 29 (2004) 1085–1104
ENERGY
www.elsevier.com/locate/energy

Availability analysis of a turbocharged diesel engine operating under transient load conditions

C.D. Rakopoulos *, E.G. Giakoumis [1]

Internal Combustion Engines Laboratory, Thermal Engineering Section, Mechanical Engineering Department, National Technical University of Athens, 9 Heroon Polytechniou Street, Zografou Campus, 15780 Athens, Greece

Received 24 July 2003

Abstract

A computer analysis is developed for studying the energy and availability performance of a turbocharged diesel engine, operating under transient load conditions. The model incorporates many novel features for the simulation of transient operation, such as detailed analysis of mechanical friction, separate consideration for the processes of each cylinder during a cycle (''multi-cylinder'' model) and mathematical modeling of the fuel pump. This model has been validated against experimental data taken from a turbocharged diesel engine, located at the authors' laboratory and operated under transient conditions. The availability terms for the diesel engine and its subsystems are analyzed, i.e. cylinder for both the open and closed parts of the cycle, inlet and exhaust manifolds, turbocharger and aftercooler. The present analysis reveals, via multiple diagrams, how the availability properties of the diesel engine and its subsystems develop during the evolution of the engine cycles, assessing the importance of each property. In particular the irreversibilities term, which is absent from any analysis based solely on the first-law of thermodynamics, is given in detail as regards transient response as well as the rate and cumulative terms during a cycle, revealing the magnitude of contribution of all the subsystems to the total availability destruction.

1. Introduction

Diesel engine simulation modeling has long been established as an effective tool for studying engine performance and contributing to evaluation and new developments. Thermodynamic

* Corresponding author. Tel.: +30-210-7723529; fax: +30-210-7723531.
E-mail address: cdrakops@central.ntua.gr (C.D. Rakopoulos).
[1] Currently with ''Lion Hellas SA'', Peugeot Automobiles Distributors, Athens, Greece.

0360-5442/$ - see front matter © 2004 Elsevier Ltd. All rights reserved.
doi:10.1016/j.energy.2004.02.028

Nomenclature

A	availability (J)
b	flow availability (J/kg)
c_p	specific heat capacity under constant pressure (J/kg K)
c_v	specific heat capacity under constant volume (J/kg K)
G	mass moment of inertia (kg m^2) or Gibbs free enthalpy (J)
g	specific Gibbs free enthalpy (J/kg)
h	specific enthalpy (J/kg)
I	irreversibility (J)
m	mass (kg)
$\dot{m}$	mass flow rate (kg/s)
N	engine speed (rpm)
p	pressure (Pa)
Q	heat (J)
R_s	specific gas constant (J/kg K)
S	entropy (J/K)
s	specific entropy (J/kg K)
T	absolute temperature (K) or torque (N m)
t	time (s)
U	internal energy (J)
V	volume (m^3)
z	fuel pump rack position (m)

Greek symbols

μ	chemical potential (J/kg)
φ	crank angle (deg or rad)
ω	angular velocity (s^{-1})

Subscripts

o	reference conditions
1	initial conditions
2	compressor outlet
3	aftercooler outlet
4	inlet manifold
5	cylinder
6	exhaust manifold
7	turbine outlet
C	compressor
ch	chemical
e	engine
em	exhaust manifold

f	fuel
fb	fuel burning
fr	friction
g	gas
i	any species
im	inlet manifold
j	any cylinder
L	load or loss
TC	turbocharger
T	turbine
tot	total
w	wall or work

Abbreviations

°CA	degrees of crank angle
rpm	revolutions per minute

models of the real diesel engine cycle [1–5] have served as effective tools for complete analysis of engine performance and sensitivity to various operating parameters.

Transient response, especially of turbocharged diesel engines, forms a significant part of their operation and is often characterized by short but serious off-design functions, requiring careful and proper modeling for successful study of the speed response. Transient diesel engine modeling extends from quasi-linear codes [3] using experimental data at steady-state conditions together with dynamic equations for the engine, turbocharger and governor, to more advanced works where the simulation is based on a detailed thermodynamic (per degree crank angle) analysis [6–12].

Moreover, during the last two decades, it has become clear that second-law (availability) analysis, with detailed study of what is happening during a process, has contributed a new way of thinking about and studying various thermodynamic engine processes [13–22]. Second-law theory introduces the term of irreversibilities, the reduction of which can lead to better engine performance, as well as the ability of increasing the overall engine efficiency by possible recovery of the work potential in the exhaust gases or heat losses. Consequently, a combined first and second-law study is required for issues concerning engine design, evaluation and performance.

Second-law research has focused on fundamental analyses [13,14,17,21] but also on irreversibilities production [16,21–25], limited-cooled engine operation [23], parametric study of speed and load effects [26], comparison between different burning fuels [27] as well as spark-ignition engines [24].

However, it should be noted that the second-law analysis has always been applied in the past to the steady-state operation of internal combustion engines. The corresponding transient operation case was dealt once in Ref. [28] by the present research group, concerning naturally aspirated engines. In this paper, the second-law analysis is extended to cover the intrinsically more complicated turbocharged engines transient operation.

For this purpose, a transient diesel engine simulation code, based on the filling and emptying modeling technique, has been developed, which incorporates some important novel features to account for the peculiarities of the transient operations. Improved relations concerning (indirect) fuel injection, combustion, dynamic analysis, heat transfer to the cylinder walls, friction modeling, fuel pump operation and turbocharger and aftercooler operation during the transient response have been developed [10–12], which contribute to a more in-depth modeling. Furthermore, a multi-cylinder engine model is incorporated, i.e. one which solves the corresponding differential equations individually for each cylinder, providing a more detailed simulation of the transient processes. The latter issue is important since, during a transient event, considerable differentiations in fueling from cylinder to cylinder inside the same cycle are observed, mainly during the first cycles.

The experimental investigation was carried out on a 6-cylinder, IDI (indirect injection), turbocharged and aftercooled, medium-high speed diesel engine of marine duty coupled to a hydraulic brake, located at the authors' laboratory. A high-speed data acquisition system was setup for measuring engine and turbocharger variables performance, under both steady-state and transient operation. The transient behavior of the engine is predicted adequately by the developed code, despite the long non-linear brake loading times and the IDI nature of the engine.

The availability balance equation is applied to the present diesel engine and all of its subsystems, i.e. compressor, aftercooler, inlet manifold, cylinder for both the closed and open parts of the cycle, exhaust manifold and turbine. Various availability properties developed during a transient event such as work, heat transfer, exhaust gas and irreversibilities are depicted in detailed multiple diagrams. In particular, the irreversibilities terms (reduced to the incoming fuel availability or total irreversibilities) for the diesel engine and its subsystems are provided for every transient cycle, for the first time. Moreover, the rate and cumulative terms of all important availability properties are given, in comparison, for the first and last cycle of the transient event. The importance of the combustion irreversibilities as well as of the exhaust manifold ones is readily revealed.

2. Energy analysis

2.1. General process description

There is a spatial uniformity of pressure, temperature and composition in the combustion chamber at each instant of time (single-zone model). The fuel is dodecane ($C_{12}H_{26}$) with a lower heating value, LHV $= 42,500$ kJ/kg. Polynomial expressions proposed by Krieger and Borman [2] are used for each of the four species (O_2, N_2, CO_2, and H_2O) considered, concerning the evaluations of internal energy and specific heat capacities for first-law applications to the engine cylinder contents [1–5,10]. The filling and emptying modeling technique is used for the simulation of all systems processes. A brief summary of the most important equations is given in Appendix A.

2.2. In-cylinder processes

For the study of the combustion process, the model proposed by Whitehouse and Way is used [2,3,10]. This model, with separate equations describing the preparation and the reaction

rate of the burning process inside the cylinder, has proven its reliability at both steady-state and transient conditions. Moreover, for a more proper simulation of transient response, the combustion modeling applied takes into consideration the continuously changing nature of operating conditions. Thus the constant K_1, in the preparation rate equation of the Whitehouse–Way model, is correlated with the Sauter mean diameter (SMD) of the fuel droplets by a formula of the type $K_1 \propto (1/\mathrm{SMD})^2$ [2]. Here, an empirical expression proposed by Hiroyasu et al. [29] is used for the evaluation of SMD at each cycle.

The model of Annand [1–3,10] is used to simulate heat loss to the cylinder walls. In particular, for transient engine operation, an hysterysis expression is used to update the wall temperature T_w at each consecutive cycle, which changes as a result of the increase in speed and/or fueling [10].

For the calculation of friction inside the cylinder, the method proposed by Rezeka and Henein [30] is adopted, which describes the non-steady profile of friction torque during each cycle. In this method, the total amount of friction is divided into six parts, i.e. ring viscous lubrication, ring mixed lubrication, piston skirt, valve train, auxiliaries and journal bearings. The important aspect about this method is that friction torque varies during each degree crank angle in the engine simulation, unlike the mean fmep (friction mean effective pressure) approaches used so far by all other researchers.

2.3. Multi-cylinder model

For the proper simulation of the transient engine performance, a multi-cylinder engine model is developed, i.e. one in which all the governing differential and algebraic equations are solved individually for every one cylinder of the 6-cylinder engine under study. At steady-state operation, the performance of each cylinder is essentially the same, due to the steady-state operation of the governor clutch resulting in the same amount of fuel injected per cycle.

At transient operation, on the contrary, each cylinder experiences different fueling during the same engine cycle due to the continuous movement of the fuel pump rack, initiated by the load or speed change. These differentiations in fueling are sometimes in the order of 10% or even more, in the same cycle, when comparing the first and the last cylinder with respect to the firing order. Thus, they can result in significant differentiations in torque response and finally speed, mainly during the early cycles, so affecting significantly the whole engine operation.

2.4. Fuel pump operation

The amount of fuel injected per cycle and cylinder is found according to the instantaneous values of engine speed and fuel pump rack position, existing at the point of static injection timing of the particular cylinder. In all the previous transient simulations, steady-state fuel pump characteristics were made use of (rack position according to speed and load). In this work, a mathematical fuel injection model is used [31] to simulate the fuel pump, providing also the dynamic injection timing and the duration of injection for each transient cycle. This constitutes a vital improvement in transient modeling, since the fueling characteristics during a transient event differ broadly compared to the steady-state curves.

3. Dynamic analysis

3.1. Engine dynamics

If G_{tot} represents the total system moment of inertia (engine, flywheel and load), then the conservation of energy principle applied to the total system (engine plus load) yields [1,10,11]:

$$T_e(\varphi,\omega) - T_L(\omega) - T_{fr}(\varphi,\omega) = G_{tot}\frac{d\omega}{dt} \tag{1}$$

where $T_e(\varphi,\omega)$ stands for the instantaneous value of the engine torque, consisting of the gas and the inertia forces torque. In the analysis, the complex (reciprocating and rotating at the same time) movement of the connecting rod is taken into consideration [11]. Also, $T_L(\omega)$ is the load torque, which, for the hydraulic brake coupled to the engine examined, is $T_L(\omega) \propto \omega^2$. Lastly, $T_{fr}(\varphi,\omega)$ stands for the friction torque, which varies during each cycle and for every cylinder according to the explicit friction analysis based on the Rezeka–Henein method [30].

3.2. Turbocharger dynamics

Accordingly, the dynamic equation for the turbocharger is [1,3,8]:

$$\eta_{mTC}\dot{W}_T - \left|\dot{W}_C\right| = G_{TC}\frac{d\omega_{TC}}{dt} \tag{2}$$

where $\dot{W}_C$ and $\dot{W}_T$ are the instantaneous values for the compressor and turbine power, respectively, while the turbocharger mechanical efficiency η_{mTC} is mainly a function of its speed.

3.3. Governor dynamics

To find the instantaneous fuel pump rack position z which is initiated by the mechanical governor clutch movement, during the transient operation, a second order differential equation is used [3,6,12]:

$$\frac{d^2z}{d\varphi^2} = c_1\frac{dz}{d\varphi} + c_2 z + c_3 z\omega^2 + c_4\omega^2 + c_5 \tag{3}$$

with constants $c_i (i = 1,\ldots,5)$ derived after calibration against experimental data under transient conditions.

4. Second-law analysis

4.1. General description

The availability of a system in a given state is defined as the maximum reversible work that can be produced through interaction of the system with its surroundings, as it reaches thermal, mechanical and chemical equilibrium [13–16,19,21]. As regards chemical equilibrium, some researchers propose that the work that could be obtained due to the difference in the partial

pressures between the system constituents at the dead state and their surroundings counterparts should also be included [13,20,21]. This work could be extracted with the use of semi-permeable membranes or other special devices such as the Van't Hoff cells. Other researchers claim that the production of this work is practically impossible, so it should not be accounted for in the calculations [15,19,23]. This approach is followed in the present study with thermal and mechanical availability terms being taken into account, while chemical availability is involved only in the reaction of fuels to form products. Since the present study concerns a diesel engine, so working at lean conditions, there are practically no partial products in the exhaust that could contain substantial chemical availability. Of course, this is unlike the case of a spark-ignition engine working at rich conditions [21].

Application of the availability balance equation to the diesel engine subsystems, on a °CA basis, yields the relations to be given in the succeeding paragraphs [13,17,21,25,26,28]. Indices 1–7 refer to the strategic points locations indicated on the schematic arrangement of the engine depicted in Fig. 1.

4.2. Cylinder

For the cylinder, we have

$$\frac{\mathrm{d}A_\mathrm{j}}{\mathrm{d}\varphi} = \frac{\dot{m}_{4\mathrm{j}} b_4 - \dot{m}_{5\mathrm{j}} b_{5\mathrm{j}}}{6N} - \frac{\mathrm{d}A_\mathrm{w}}{\mathrm{d}\varphi} - \frac{\mathrm{d}A_\mathrm{L}}{\mathrm{d}\varphi} + \frac{\mathrm{d}A_\mathrm{f}}{\mathrm{d}\varphi} - \frac{\mathrm{d}I}{\mathrm{d}\varphi} \tag{4}$$

with $\dot{m}_{4\mathrm{j}}$ the incoming flow rate from the inlet manifold and $\dot{m}_{5\mathrm{j}}$ the outgoing one to the exhaust manifold for the particular cylinder j according to the energy analysis:

$$\frac{\mathrm{d}A_\mathrm{w}}{\mathrm{d}\varphi} = (p_{5\mathrm{j}} - p_\mathrm{o}) \frac{\mathrm{d}V}{\mathrm{d}\varphi} \tag{5}$$

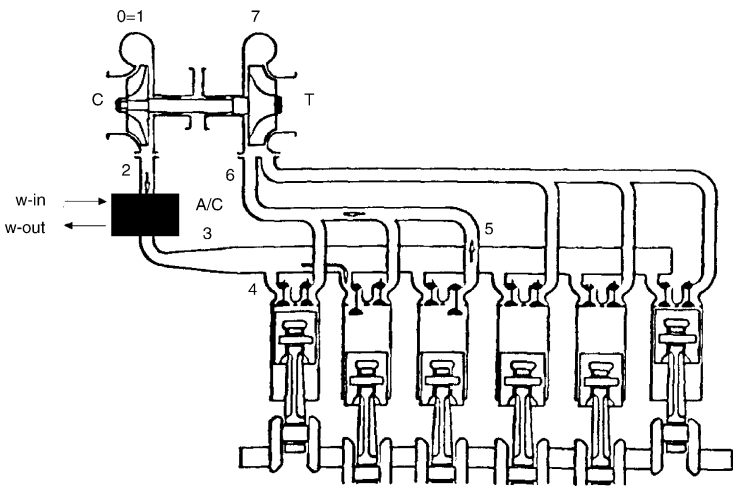

Fig. 1. Schematic arrangement of the diesel engine, manifolds, turbocharger and aftercooler.

is the work transfer, where $\mathrm{d}V/\mathrm{d}\varphi$ is the rate of change of cylinder volume with crank angle and $p_{5\mathrm{j}}$ the instantaneous cylinder pressure:

$$\frac{\mathrm{d}A_{\mathrm{L}}}{\mathrm{d}\varphi}=\frac{\mathrm{d}Q_{\mathrm{L}}}{\mathrm{d}\varphi}\left(1-\frac{T_{\mathrm{o}}}{T_{5\mathrm{j}}}\right) \tag{6}$$

is the heat transfer to the cylinder walls (considered here as external to the cylinder control volume) with $\mathrm{d}Q_{\mathrm{L}}/\mathrm{d}\varphi$ given by the Annand correlation, and $T_{5\mathrm{j}}$ the instantaneous cylinder gas temperature:

$$\frac{\mathrm{d}A_{\mathrm{f}}}{\mathrm{d}\varphi}=\frac{\mathrm{d}m_{\mathrm{fb}}}{\mathrm{d}\varphi}a_{\mathrm{fch}} \tag{7}$$

is the injected fuel availability, with a_{fch} being the (chemical) availability associated with burning of liquid hydrocarbon fuels of the type $\mathrm{C}_m\mathrm{H}_n$ and is given by Moran [13]:

$$a_{\mathrm{fch}}=\mathrm{LHV}\left(1.04224+0.011925\frac{n}{m}-\frac{0.042}{m}\right) \tag{8}$$

For the present analysis, $m=12$, $n=26$ and $a_{\mathrm{fch}}=1.064$ LHV. The fuel burning rate $\mathrm{d}m_{\mathrm{fb}}/\mathrm{d}\varphi$ is calculated, for each computational step, with the use of the Whitehouse–Way model. The term on the lhs of Eq. (4) is expressed explicitly as

$$\frac{\mathrm{d}A_{\mathrm{j}}}{\mathrm{d}\varphi}=\frac{\mathrm{d}U_{\mathrm{j}}}{\mathrm{d}\varphi}+p_{\mathrm{o}}\frac{\mathrm{d}V_{\mathrm{j}}}{\mathrm{d}\varphi}-T_{\mathrm{o}}\frac{\mathrm{d}S_{\mathrm{j}}}{\mathrm{d}\varphi}-\frac{\mathrm{d}G_{\mathrm{oj}}}{\mathrm{d}\varphi} \tag{9}$$

representing the change in the availability of the contents of cylinder j under consideration. Details about the derivation of terms U, S, and G_{o} are given in Appendix A.

The terms b_4 and b_5 in Eq. (4) refer to the flow availability of the incoming and the outgoing cylinder mass flow rate, respectively, defined as [13]:

$$b=h-h_{\mathrm{o}}-T_{\mathrm{o}}(s-s_{\mathrm{o}}) \tag{10}$$

The term $\mathrm{d}I/\mathrm{d}\varphi$ in Eq. (4) is the rate of irreversibility production within the cylinder which consists mainly of the combustion term, while inlet-valve throttling and mixing of the incoming air with the cylinder residuals contribute a little.

4.3. Compressor

For the compressor, no control volume exists and the availability balance equation reads

$$\frac{\dot{m}_1 b_1-\dot{m}_2 b_2}{6N}+\frac{\dot{W}_{\mathrm{C}}}{6N}=\frac{\mathrm{d}I_{\mathrm{C}}}{\mathrm{d}\varphi} \tag{11}$$

with $\dot{m}_1=\dot{m}_2$ the charge air flow rate.

4.4. Aftercooler

For the aftercooler (IC), similarly, the availability balance equation is

$$\frac{\dot{m}_2 b_2 - \dot{m}_3 b_3}{6N} - \Delta A_w = \frac{dI_{IC}}{d\varphi} \tag{12}$$

where b_2 is the flow availability at the compressor outlet–aftercooler inlet, b_3 the flow availability at the aftercooler outlet–inlet manifold inlet, and

$$\Delta A_w = \frac{\dot{m}_w c_{pw}[T_{w\text{-out}} - T_{w\text{-in}} - T_o \ln(T_{w\text{-out}}/T_{w\text{-in}})]}{6N} \tag{13}$$

is the increase in the availability of the cooling medium [13] having mass flow rate $\dot{m}_w$, specific (mass) heat capacity c_{pw}, initial temperature entering the aftercooler $T_{w\text{-in}}$ and final temperature leaving the aftercooler $T_{w\text{-out}}$. Here, the irreversibilities account for the loss of availability due to the transfer of heat to a cooler medium (a very small amount of destroyed availability, as will be shown in Fig. 7). This is a procedure not desirable according to the second-law of thermodynamics, although from the first-law perspective it is of particular importance for the increase of the output of the engine (increase of volumetric efficiency).

4.5. Inlet manifold

For the inlet manifold, the availability balance equation is

$$\frac{dA_{im}}{d\varphi} = \frac{\dot{m}_3 b_3 - \sum_{j=1}^{6} \dot{m}_{4j} b_4}{6N} - \frac{dI_{im}}{d\varphi} \tag{14}$$

where b_4 is the flow availability at the intake-manifold and $j = 1, \ldots, 6$ the cylinder exchanging mass with the inlet manifold found from the energy analysis at each degree crank angle. The term for irreversibilities $dI_{im}/d\varphi$ accounts mainly for the mixing of incoming air with the intake-manifold contents.

4.6. Exhaust manifold

For the exhaust manifold, the availability balance equation is

$$\frac{dA_{em}}{d\varphi} = \frac{\sum_{j=1}^{6} \dot{m}_{5j} b_{5j} - \dot{m}_6 b_6}{6N} - \frac{dI_{em}}{d\varphi} + \frac{dA_{Lem}}{d\varphi} \tag{15}$$

where index 6 identifies the exhaust manifold state. The term

$$\frac{dA_{Lem}}{d\varphi} = \frac{dQ_{Lem}}{d\varphi}\left(1 - \frac{T_o}{T_6}\right) \tag{16}$$

accounts for heat losses at the exhaust manifold (considered as external to the manifold control volume, thus not included in the respective irreversibilities), where T_6 is the instantaneous temperature of the manifold contents. The term $dI_{em}/d\varphi$ is the irreversibility rate in the exhaust

manifold, which arises from throttling across the exhaust valve, mixing of cylinder exhaust gases with manifold contents and friction along the manifold length.

The $dA/d\varphi$ terms given in the previous equations for the cylinder and the manifolds are evaluated according to Eq. (9); for unsteady operations they do not sum up to zero (as they do for steady-state operation) at the end of a full cycle of the working medium. Their respective cumulative values $\int(dA/d\varphi)\,d\varphi$ are, however, small (not more than 0.40% of the incoming fuel's availability) compared to the other availability terms, due to the large total moment of inertia of the examined engine-brake system, which slows down the reaction of the fuel pump rack and consequently the speed response of the engine.

4.7. Turbine

For the turbine, the availability balance equation is

$$\frac{\dot{m}_6 b_6 - \dot{m}_7 b_7}{6N} - \dot{W}_T = \frac{dI_T}{d\varphi} \tag{17}$$

with 7 denoting the state of the gases leaving the turbine to the atmosphere.

All the equations for the energy and availability simulation are solved for every $1/4^{\circ}$CA for the closed part of each cycle, or every $1/2^{\circ}$CA for the open part. The dynamic ones are solved once every degree crank angle for the diesel engine and every 120°CA for the turbocharger.

5. Experimental facilities and measurements

The objective of the experimental test bed developed was to validate the transient performance of the engine simulation. To accomplish this task, the engine was coupled to a hydraulic brake (dynamometer). The basic data for the engine, turbocharger, brake and data processing system are shown in Table 1.

Table 1
Basic data for engine, turbocharger, dynamometer and data logging system

Engine model and type	MWM TbRHS 518S in-line, 6-cylinder, 4-stroke, compression ignition, IDI, turbocharged, aftercooled, marine duty
Speed range	1000–1500 rpm
Bore/stroke	140/180 mm
Compression ratio	17.7
Maximum power	320 hp (236 kW) at 1500 rpm
Maximum torque	1520 N m at 1250 rpm
Total moment of inertia (engine, flywheel and brake)	15.60 kg m^2
Brake model and type	Schenck U1-40, hydraulic brake
Turbocharger moment of inertia	7.5×10^{-4} kg m^2
Data logging system	Two 12-bit, 8-channel ADCs, 100 kHz max. sampling rate, installed on IBM compatible PCs

The experimental investigation was conducted on an MWM TbRHS 518S, 6-cylinder, turbocharged and aftercooled, IDI, medium-high speed diesel engine of marine duty. The engine is fitted with a Kuehnle, Kopp and Kausch (KKK) turbocharger and a water aftercooler (a/c) after the turbocharger compressor. It is fitted with a variable-speed mechanical governor. The engine is permanently coupled to a Schenck hydraulic dynamometer. This is a variable fill brake, with the loading accomplished via the brake lever, which controls the amount of water swirling inside the machine. Details about the experimental setup can be found in Ref. [12].

Since the particular engine is one with a relatively small speed range, mainly load changes (increases), with constant governor setting, commencing from various initial engine speeds were examined. These were used to validate the model's accuracy at transient conditions.

6. Results and discussion

A typical example of a conducted transient experiment is given in Fig. 2. Here, the initial load was 10% of the full engine load at 1180 rpm. The final load applied was almost 75% of the full engine load; it was applied in 0.2 s.

The application of the final load was effected by the movement of the brake control lever (this task lasted 0.2 s), which in turn increased the amount of water inside the brake by appropriately increasing the active surface of the inlet tube. However, this hydraulic brake is characterized by

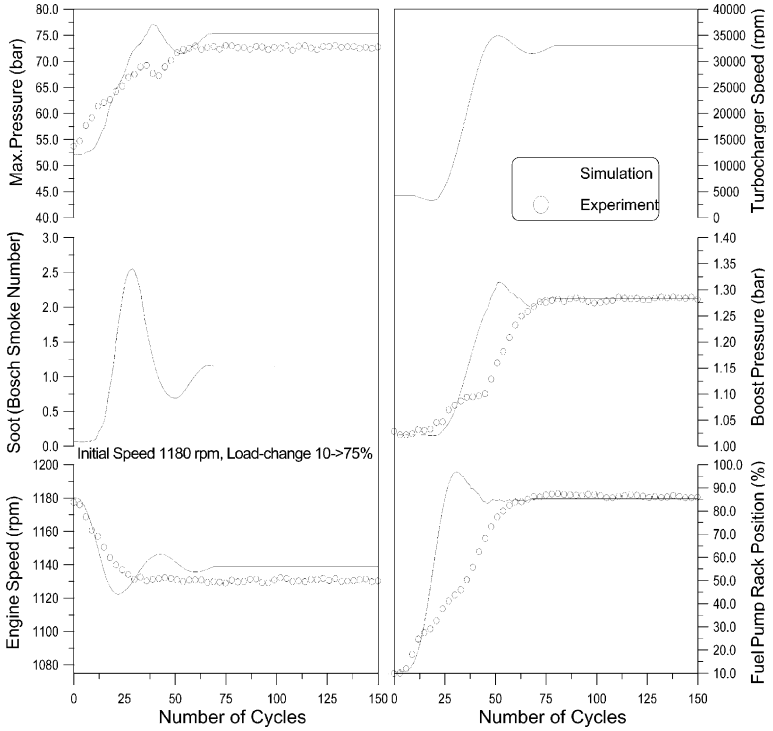

Fig. 2. Predicted and experimental engine energy response to an increase in load.

a high mass moment of inertia, in the order of 5.375 kg m^2, resulting in long and non-linear actual load-change times. This phenomenon was accounted for in the simulation model by arbitrarily increasing the load appliance time. The overall matching between experimental and predicted transient responses seems to be satisfactory for both engine and turbocharger variables (engine speed, maximum pressure for main chamber, fuel pump rack position and boost pressure).

We also provide in Fig. 2, turbocharger speed and soot emission variations. The prediction of soot given here should be seen with caution, since a single-zone model is not capable of predicting it accurately. A simple expression of the type $BSN = s_1\, e^{s_2 AFR}$ has been used, where BSN is the Bosch Smoke Number of the current cycle, with the constants s_1 and s_2 derived after calibration against experimental data at steady-state conditions, and AFR is the corresponding cycle air to fuel mass ratio.

The predicted availability response of the engine and its subsystems for the particular load-change is depicted in the following diagrams.

Fig. 3 shows the response of the in-cylinder availability terms, viz., work, heat loss to the walls, exhaust gas and irreversibilities as a function of the engine cycles. All of these terms are cumulative values (J) over each cycle (for cylinder no. 1 of the engine). The availability term for work and heat loss to the walls increase with the increase in fueling as a function of the engine cycles, because of increases in the charge temperature resulting from increases of the injected fuel quantities and accompanying fuel–air equivalence ratios. Similar results hold for the exhaust gas from the cylinder term and for the irreversibilities term.

Fig. 4 examines the same in-cylinder properties, but now their values are reduced to the cylinder's fuel availability over each cycle. Here, we see that the reduced availability term for heat loss to the walls initially increases with the increase in fueling, but subsequently decreases and finally returns to the initial value of almost 18% of the fuel availability, owing to the greater increases of the other terms. The response of the heat loss term shows an hysterysis compared

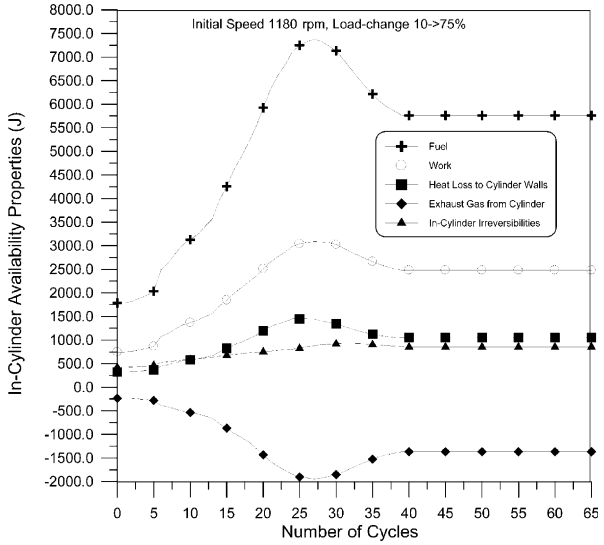

Fig. 3. Response of cylinder availability properties to an increase in load.

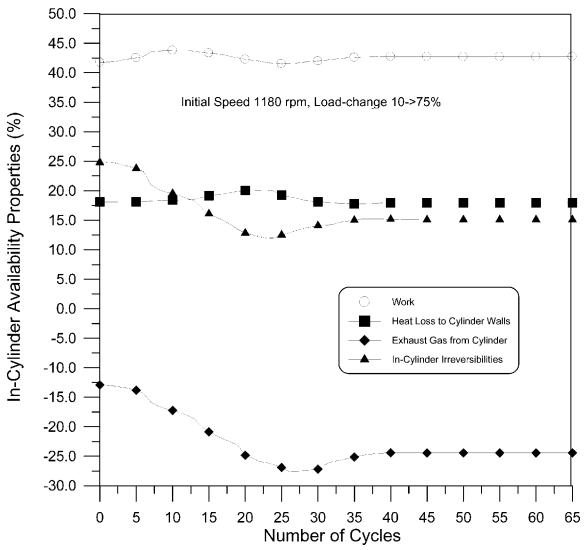

Fig. 4. Response of cylinder availability properties, reduced to the fuel availability, to an increase in load.

to the work one, although it should be noted that the maximum change in the reduced values is in the order of 2 percentage points, or approximately 10%, compared to the peak value observed at cycle 23. The absolute value of the reduced term of exhaust gases leaving the cylinder (corresponding mass flow rate $\dot{m}_{5j}$ and flow availability b_5 in Eq. (4)), on the other hand, increases steadily with the increase in fueling as the transient event develops. The reduced in-cylinder irreversibilities decrease due to the fact that combustion irreversibilities fall with increasing load [26]. Greater loads result in less degradation of fuel chemical availability when transferred to the (hotter) exhaust gases and also less mixing of exhaust gases with the air.

Fig. 5 deconvolutes the irreversibilities terms (J) inside the cylinder, i.e. combustion, inlet and exhaust ones. The dominant role of the combustion irreversibilities is shown here (at least 95% of the total cylinder ones), having an increasing importance as the transient event develops, i.e. with increase in fueling. Their greatest part is produced at the early stage of combustion where the gas temperature is still low. The inlet irreversibilities account for throttling across the inlet valve, which in any case are small due to the relatively low pressure and temperature of the inlet gas. It must be noted here, that the irreversibilities due to the throttling across the exhaust valve are accounted for in the exhaust manifold irreversibilities.

Fig. 6 shows the response of the total irreversibilities, i.e. of cylinders plus manifolds plus aftercooler plus turbocharger, reduced to the total injected fuel availability. Owing to the great contribution of the combustion irreversibilities, the total ones show a similar transient profile with those of the in-cylinder ones depicted in Fig. 4, i.e. they decrease as the load increases with the minimum value occurring at cycle 23.

Fig. 7 concentrates on the irreversibilities terms of the various subsystems, reduced now to the total irreversibilities. Here, we show how cylinder as well as inlet manifold, exhaust manifold, compressor, turbine, and aftercooler irreversibilities develop according to the evolution of

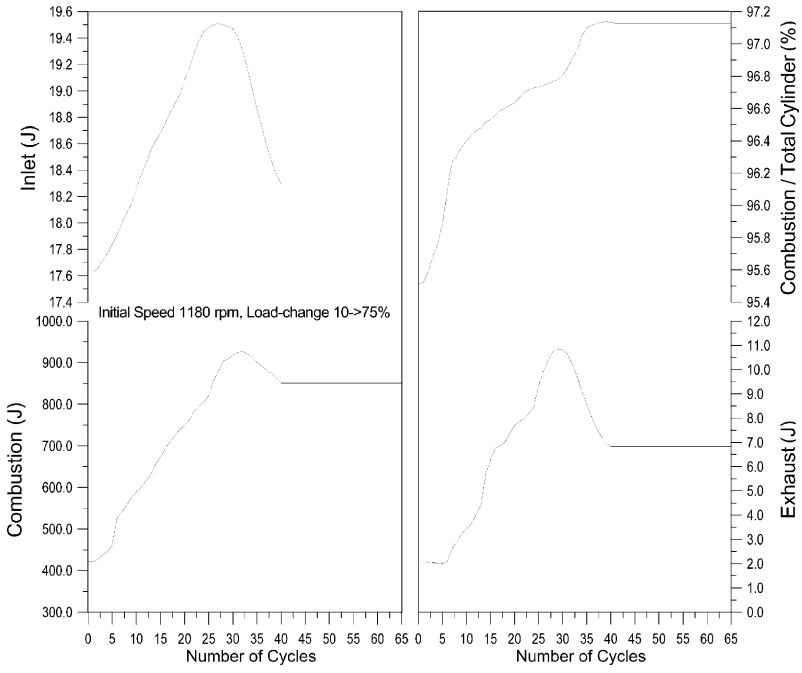

Fig. 5. Response of various in-cylinder irreversibilities to an increase in load.

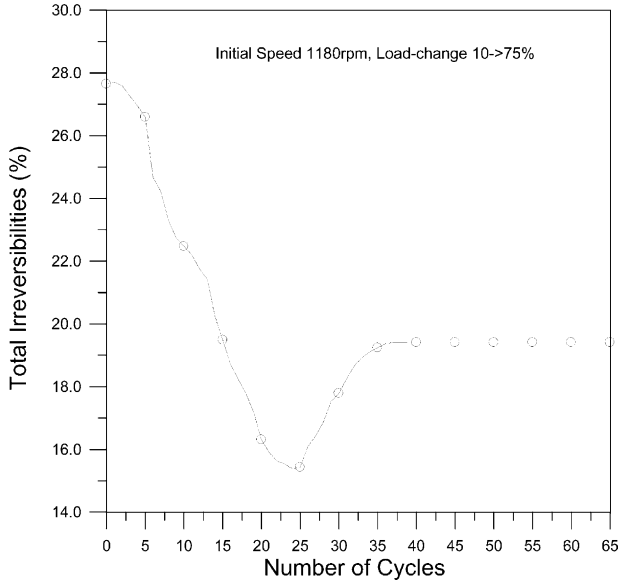

Fig. 6. Response of total irreversibilities term, reduced to the fuel availability, to an increase in load.

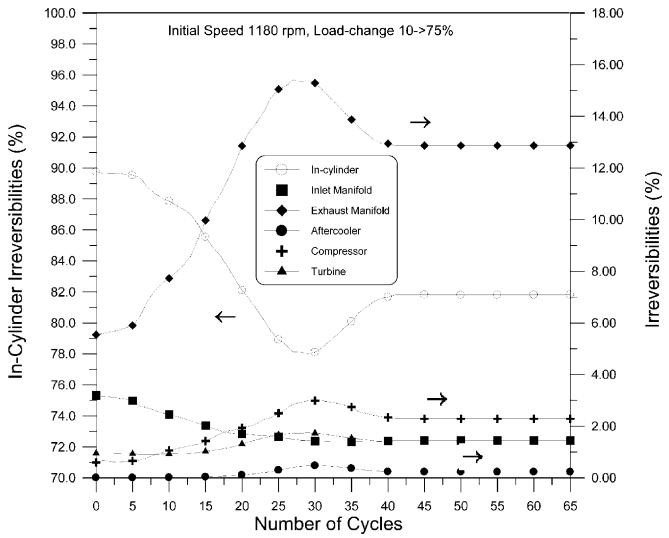

Fig. 7. Response of various diesel engine and its subsystems irreversibilities terms, reduced to the total irreversibilities, to an increase in load.

engine cycles. The relative importance of the cylinder irreversibilities decrease as the transient event develops (cf. Fig. 4), due to the increase in loading and thus fueling. The inlet manifold irreversibilities constitute a very small percentage of the total ones (not greater than 3% and with decreasing relative importance during the transient event), whereas those of the exhaust manifold increase substantially from cycle 10 where the main increase in the injected fuel quantity (and thus gas pressures and temperatures) occurs, reaching as much as 15% of the total irreversibilities at cycle 31. Turbocharger irreversibilities increase during the transient event due to the increase in both compressor and turbine pressure and temperature, accounting for 4.7% of the total irreversibilities at cycle no. 28. The compressor irreversibilities outweigh the turbine ones, except for the first cycles where the turbine isentropic efficiency is lower. Aftercooler irreversibilities never exceed 0.47% of the total ones (cycle no. 30), proving the low importance of this process as well as the very low potential for work recovery. It is also interesting to note, that the cycle where the maximum (or minimum) percentage occurs differs for every subsystem. This is due to the different "inertia" of each subsystem, which differentiates also its transient response.

Fig. 8 concentrates on the first and the last cycle of the particular transient operation, showing the development in the rate of the various availability terms (J/°CA), i.e. cylinder (Eq. (9)), fuel, work, heat loss to the walls, irreversibilities (all for cylinder no. 1), exhaust gas to ambient, exhaust manifold irreversibilities and turbine irreversibilities. Similarly, Fig. 9 focuses on the first and the last cycle of the particular transient operation, providing the development of the respective cumulative availability terms (J). Here, compared to Fig. 8, the inlet manifold as well as the compressor cumulative irreversibilities terms are depicted. The pulsating form deriving from the six cylinders contribution is obvious as regards properties of manifolds and turbocharger. Cylinder cumulative availability, as expected, sums up to zero after the 720°CA of

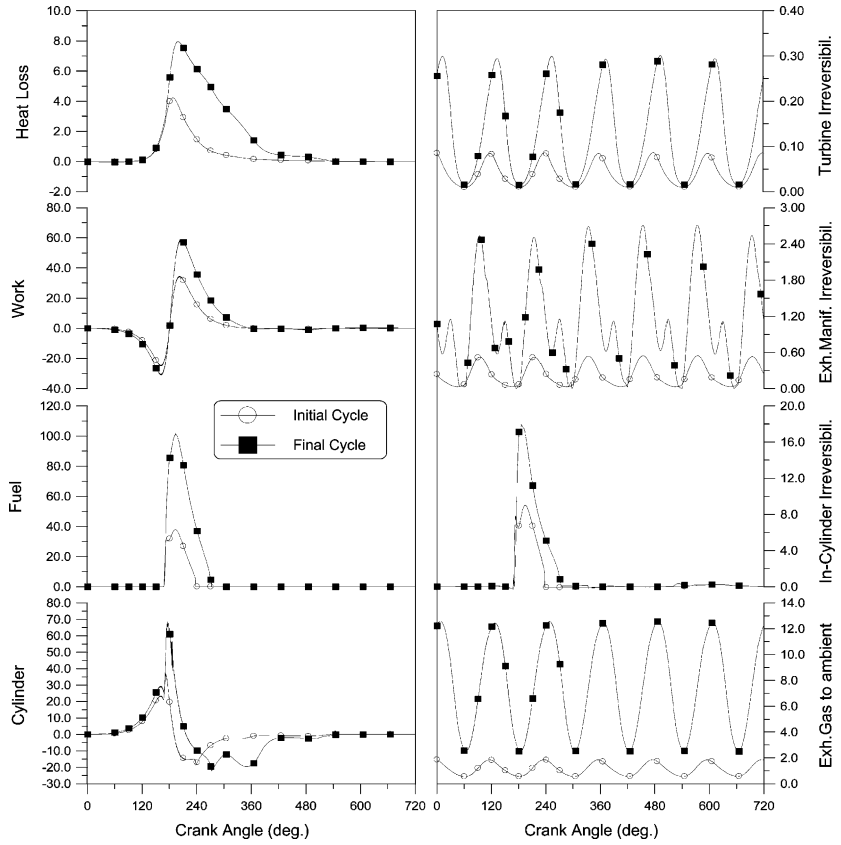

Fig. 8. Development in the rate (J/°CA) of availability terms of diesel engine and its subsystems, at the initial and final steady-state conditions.

the first or the last cycle. Both the fuel and the combustion irreversibility profiles develop in a similar way.

7. Conclusion

A detailed second-law analysis has been carried out on a 6-cylinder, turbocharged diesel engine to study the availability performance of all engine subsystems during transient operation, after a load-change commencing from a low load. The model's energy results are confirmed with experimental tests.

The availability term for the heat loss to the cylinder walls increases substantially during the transient event (increased potential for work recovery), but the reduced term returns to the initial value after a peak in the middle of the transient event. The availability of the exhaust gases from the cylinder increase significantly after an increase in load (increased potential for work recovery).

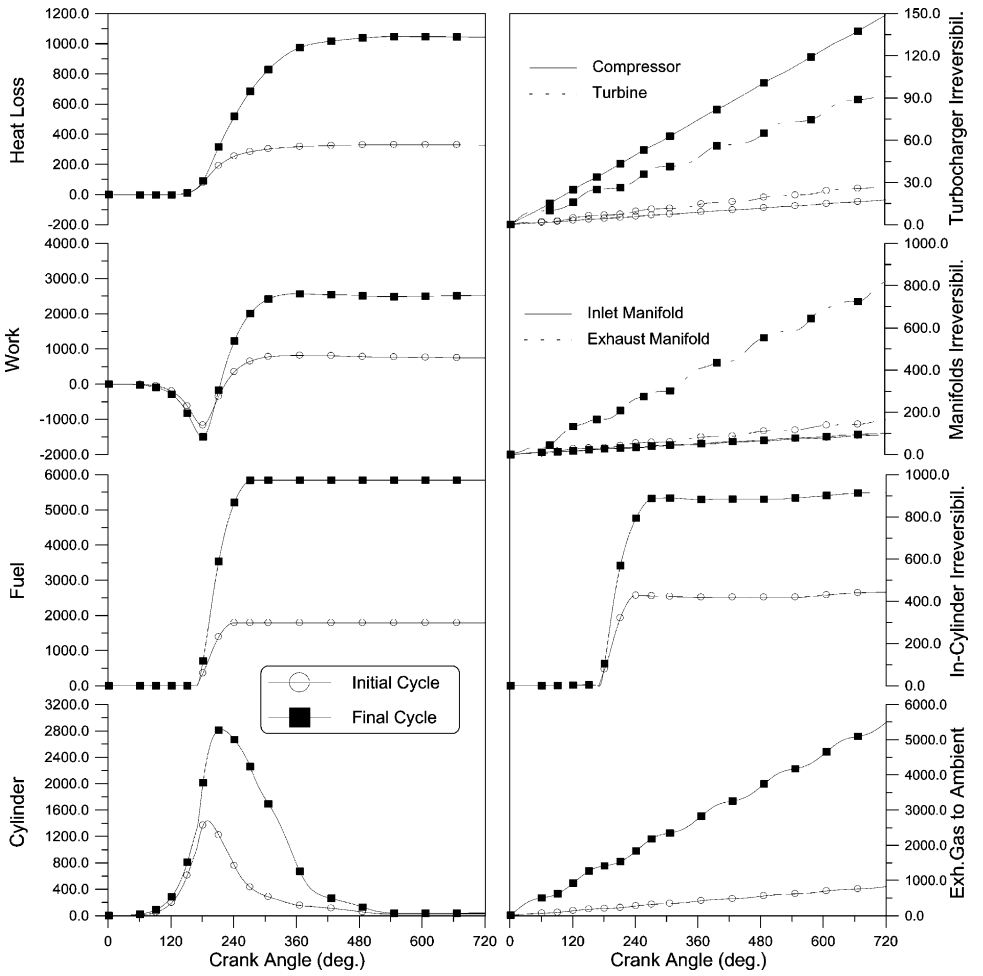

Fig. 9. Development in the cumulative (J) availability terms of diesel engine and its subsystems, at the initial and final steady-state conditions.

Cylinder irreversibilities decrease, proportionally, after a ramp increase in load due to the subsequent increase in fueling, while combustion irreversibilities account for at least 95% of the total cylinder ones. Every operating parameter that can decrease the amount of combustion irreversibilities (e.g. greater cylinder wall temperature) is favorable according to second-law and can lead to increased piston work.

Exhaust manifold irreversibilities increase significantly during a load increase, reaching as high as 15% of the total ones, highlighting another process which needs to be studied for possible efficiency improvement. This increased amount of irreversibilities arises mainly from the greater pressures and temperatures due to turbocharging, which have already lowered the reduced magnitude of combustion irreversibilities. The inlet manifold irreversibilities, on the other hand, are of lesser and decreasing importance during the transient event.

Turbocharger irreversibilities, though only a fraction of the (dominant) combustion ones, are not negligible, while the intercooler irreversibilities steadily remain of lesser importance (less than 0.5% of the total ones) during a load change.

The cycle where each (reduced) availability term presents its peak is different for every subsystem.

Appendix A

For the Whitehouse–Way [2] combustion model, the preparation limited combustion rate P (kg of fuel per °CA) is

$$P = K_1 M_i^{1-x} M_u^x p_O^y \tag{A.1}$$

which controls the burned fuel for the larger part of combustion, while for the reaction rate R (kg of fuel per °CA) which is responsible for the early part of combustion it holds

$$R = \frac{K_2 p_O}{N\sqrt{T}} e^{-act/T} \int (P - R)\, d\varphi \tag{A.2}$$

where $M_i = \int (dm_{fi}/d\varphi)\, d\varphi$ is the total mass (kg) of injected fuel up to the crank angle φ considered, and $(dm_{fi}/d\varphi)$ is the injection rate found from the analytical fuel injection model. $M_u = M_i - \int P\, d\varphi$ is the total mass (kg) of unprepared fuel, "act" is the reduced activation energy (K) accounting for the ignition delay and p_O is the partial pressure of oxygen (bar) in the main chamber or the prechamber.

The heat loss Q_L to cylinder walls is given by the model of Annand [2]:

$$\frac{dQ_L}{dt} = F_p \left[\alpha\lambda Re^{\beta}(T_w - T_g)/D + \gamma\left(T_w^4 - T_g^4\right)\right] \tag{A.3}$$

where $F_p = 2\pi D^2/4 + \pi D x$ is the surface and x the instantaneous cylinder height in contact with the gas, λ is the gas thermal conductivity (W/m K), the Reynolds number Re is calculated with a characteristic speed equal to the mean piston speed and a characteristic length equal to the piston diameter D, and α, β, γ are constants determined after matching with experimental data at steady-state conditions.

For the evaluation of internal energy, we have [25,26]:

$$\frac{dU}{d\varphi} = \sum_{i=1}^{4} u_i \frac{dm_i}{d\varphi} + \sum_{i=1}^{4} m_i c_{vi} \frac{dT}{d\varphi} \tag{A.4}$$

where m_i is the mass of species i (O_2, N_2, CO_2, and H_2O) and c_v is the specific heat capacity under constant volume (a function of temperature only $c_v = du/dT$), with

$$u_i = u_i(T) + u_{0i} \tag{A.5}$$

where the constants for the fourth order polynomial relation $u_i(T)$ can be found in Benson and Whitehouse [2], and u_{0i} is the internal energy at absolute zero.

Similarly, the rate of entropy change of the cylinder contents in Eq. (9) is

$$\frac{\mathrm{d}S}{\mathrm{d}\varphi} = \sum_{i=1}^{4} \frac{\mathrm{d}m_\mathrm{i}}{\mathrm{d}\varphi} s_\mathrm{i}(T, x_\mathrm{i}p) + \sum_{i=1}^{4} \frac{m_\mathrm{i}}{T} c_\mathrm{pi} \frac{\mathrm{d}T}{\mathrm{d}\varphi} - \frac{V}{T} \frac{\mathrm{d}p}{\mathrm{d}\varphi} \tag{A.6}$$

with

$$s_\mathrm{i}(T, x_\mathrm{i}p) = s'_\mathrm{i}(T, p_\mathrm{o}) - R_\mathrm{s}\ln\left(\frac{x_\mathrm{i}p}{p_\mathrm{o}}\right) \tag{A.7}$$

and $s'_\mathrm{i}(T, p_\mathrm{o})$ a function of temperature only, with x_i the molar fraction of species i in the mixture.

For the Gibbs free enthalpy

$$\frac{\mathrm{d}G_\mathrm{o}}{\mathrm{d}\varphi} = \sum_{i=1}^{4} \frac{\mathrm{d}m_\mathrm{i}}{\mathrm{d}\varphi} \mu_\mathrm{i}^\mathrm{o} \tag{A.8}$$

where $\mu_\mathrm{i}^\mathrm{o} = g_\mathrm{i}(T_\mathrm{o}, x_\mathrm{i}p_\mathrm{o})$ is the chemical potential of species i at ambient conditions, with

$$g_\mathrm{i}(T_\mathrm{o}, x_\mathrm{i}p_\mathrm{o}) = h_\mathrm{i}(T_\mathrm{o}) - T_\mathrm{o}s_\mathrm{i}(T_\mathrm{o}, x_\mathrm{i}p_\mathrm{o}) = h_\mathrm{i}(T_\mathrm{o}) - T_\mathrm{o}\left[s'_\mathrm{i}(T_\mathrm{o}, p_\mathrm{o}) - R_\mathrm{s}\ln(x_\mathrm{i})\right] \tag{A.9}$$

References

[1] Heywood JB. Internal combustion engine fundamentals. New York: McGraw-Hill; 1988.
[2] Benson RS, Whitehouse ND. Internal combustion engines. Oxford: Pergamon Press; 1979.
[3] Horlock JH, Winterbone DE. The thermodynamics and gas dynamics of internal combustion engines vol. II. Oxford: Clarendon Press; 1986.
[4] Rakopoulos CD, Hountalas DT. Development and validation of a 3-D multi-zone combustion model for the prediction of DI diesel engines performance and pollutants emissions. Trans SAE J Engines 1998;107:1413–29.
[5] Rakopoulos CD, Hountalas DT. Development of new 3-D multi-zone combustion model for indirect injection diesel engines with a swirl type prechamber. Trans SAE J Engines 2000;109:718–33.
[6] Watson N, Marzouk M. A non-linear digital simulation of turbocharged diesel engines under transient conditions. SAE paper no. 770123. Warrendale (PA): Society of Automotive Engineers Inc; 1977.
[7] Winterbone DE, Benson RS, Mortimer AG, Kenyon P, Stotter A. Transient response of turbocharged diesel engines. SAE paper no. 770122. Warrendale (PA): Society of Automotive Engineers Inc; 1977.
[8] Watson N. Transient performance simulation and analysis of turbocharged diesel engines. SAE paper no. 810338. Warrendale (PA): Society of Automotive Engineers Inc; 1981.
[9] Bazari Z. Diesel exhaust emissions prediction under transient operating conditions. SAE paper no. 940666. Warrendale (PA): Society of Automotive Engineers Inc; 1994.
[10] Rakopoulos CD, Giakoumis EG. Simulation and analysis of a naturally aspirated, indirect injection diesel engine under transient conditions comprising the effect of various dynamic and thermodynamic parameters. Energy Convers Mgmt 1998;39:465–84.
[11] Rakopoulos CD, Giakoumis EG, Hountalas DT. A simulation analysis of the effect of governor technical characteristics and type on the transient performance of a naturally aspirated IDI diesel engine. Trans SAE J Engines 1997;106:905–22.
[12] Rakopoulos CD, Giakoumis EG, Hountalas DT. Experimental and simulation analysis of the transient operation of a turbocharged multi-cylinder IDI diesel engine. Energy Res 1998;22:317–31.
[13] Moran MJ. Availability analysis: a guide to efficient energy use. New Jersey: Prentice-Hall; 1982.

[14] Bejan A, Tsatsaronis G, Moran M. Thermal design and optimization. New York: John Wiley and Sons Inc; 1996.
[15] Bozza F, Nocera R, Senatore A, Tuccilo R. Second law analysis of turbocharged engine operation. Trans SAE J Engines 1991;100:547–60.
[16] Dunbar WR, Lior N. Sources of combustion irreversibility. Combust Sci Technol 1994;103:41–61.
[17] Dunbar WR, Lior N, Gaggioli RA. The component equations of energy and exergy. Trans ASME J Energy Res Technol 1992;114:75–83.
[18] Dunbar WR, Lior N, Gaggioli RA. Combining fuel cells with fuel-fired plants for improved exergy efficiency. Energy 1991;16:1259–74.
[19] Flynn PF, Hoag KL, Kamel MM, Primus RJ. A new perspective on diesel engine evaluation based on second law analysis. SAE paper no. 840032. Warrendale (PA): Society of Automotive Engineers Inc; 1984.
[20] McKinley TL, Primus RJ. An assessment of turbocharging systems for diesel engines from first and second law perspectives. Trans SAE J Engines 1988;97:1061–71.
[21] Van Gerpen JH, Shapiro HN. Second-law analysis of diesel engine combustion. Trans ASME J Eng Gas Turbines Power 1990;112:129–37.
[22] Beretta GP, Keck JC. Energy and entropy balances in a combustion chamber. Combust Sci Technol 1983;30: 19–29.
[23] Rakopoulos CD, Andritsakis EC, Kyritsis DK. Availability accumulation and destruction in a DI diesel engine with special reference to the limited cooled case. Heat Recov Syst CHP 1993;13:261–75.
[24] Rakopoulos CD. Evaluation of a spark ignition engine cycle using first and second-law analysis techniques. Energy Convers Mgmt 1993;33:1299–314.
[25] Rakopoulos CD, Giakoumis EG. Development of cumulative and availability rate balances in a multi-cylinder turbocharged IDI diesel engine. Energy Convers Mgmt 1997;38:347–69.
[26] Rakopoulos CD, Giakoumis EG. Speed and load effects on the availability balances and irreversibilities production in a multi-cylinder turbocharged diesel engine. Appl Therm Eng 1997;17:299–314.
[27] Rakopoulos CD, Kyritsis DK. Comparative second-law analysis of internal combustion engine operation for methane, methanol, and dodecane fuels. Energy 2001;26:705–22.
[28] Rakopoulos CD, Giakoumis EG. Simulation and exergy analysis of transient diesel engine operation. Energy 1997;22:875–86.
[29] Hiroyasu H, Kadota T, Arai M. Development and use of a spray combustion modeling to predict diesel engine efficiency and pollutant emissions. Bull JSME 1983;26:569–76.
[30] Rezeka SK, Henein NA. A new approach to evaluate instantaneous friction and its components in internal combustion engines. SAE paper no. 840179. Warrendale (PA): Society of Automotive Engineers Inc; 1984.
[31] Kouremenos DA, Rakopoulos CD, Hountalas DT, Kotsiopoulos PN. A simulation technique for the fuel injection system of diesel engines. Proceedings of the ASME-WAM, AES, Atlanta, GA, vol. 24. 1991, p. 91–102.